

Remarkable photocurrent in heterojunctions of $n\text{-La}_{0.9}\text{Hf}_{0.1}\text{MnO}_3/i\text{-SrTiO}_3/p\text{-Si}$ at room temperature

Xiangbo Liu,¹ Libin Jin,¹ Huibin Lu,^{2,a)} and Ju Gao^{1,a)}

¹Department of Physics, The University of Hong Kong, Pokfulam Road, Hong Kong, China

²Beijing National Laboratory for Condensed Matter Physics, Institute of Physics, Chinese Academy of Sciences, Beijing 100190, China

(Received 19 November 2015; accepted 10 April 2016; published online 25 April 2016)

Controllable manipulation for electrical transport in manganite-based heterojunctions have been desired and studied all the time due to their promising applications in electronic and spintronic devices. We report heterojunctions composed by n -type $\text{La}_{0.9}\text{Hf}_{0.1}\text{MnO}_3$ and p -type Si with a SrTiO_3 interlayer. The junctions reveal the formation of n - i - p junction in a wide temperature range of 20–300 K. Under illumination of 630 nm light, remarkable photocurrent has been observed. The photosensitivity (I_S), defined as the ratio of photocurrent to dark current, reaches over 1200% under -3 V bias and illumination of red light with 10 mW cm^{-2} at room temperature. Even light power density is as low as 0.2 mW cm^{-2} , I_S is still over 200% under -1.5 V bias. The injection of photo-carriers could be responsible for the observed phenomenon. Such manipulative features by light illumination and bias should be of great potential for functional light sensors. *Published by AIP Publishing.*
[\[http://dx.doi.org/10.1063/1.4947284\]](http://dx.doi.org/10.1063/1.4947284)

As one of the most famous strongly correlated systems, lanthanum manganite (LaMnO_3) has attracted extensive attentions. LaMnO_3 is an antiferromagnetic insulator with a bandgap of ~ 1.1 eV, but artificial doping endows it rich properties, such as ferromagnetism, magnetoresistance, semimetal, metal-insulator transition.^{1–4} Much effort has been devoted to developing manganite-based devices in recent years. Among them, manganite-contained heterojunctions get extra interests for potential applications in diodes, photodetectors, solar cells, etc.^{5–7} The incorporation of manganite and silicon composes a perfect heterojunction system since we can modify the properties by introducing different ions into manganite according to our requirements. On the other hand, the electrical transport of manganite is very sensitive to external magnetic field, light illumination, temperature, and pressure because of double exchange interaction, John-Teller effect, and crystal field effect.^{6,8–10} As a result, we are able to tune the properties of manganite/Si heterojunctions easily. Nowadays, the growth technique for high quality p - and n -type Si is highly ripe. As for LaMnO_3 , A-site doping is a common method to modify the concentration of carrier in $\text{La}_{1-x}\text{D}_x\text{MnO}_3$ ($\text{D} = \text{dopant}$). P -type LaMnO_3 can be obtained by doping monovalent and bivalent ions (Na^+ , K^+ , Sr^{2+} , Ca^{2+} , Ba^{2+} , etc.). They are frequently applied into p - n junctions working as hole-conductive layers. P -manganite/ n -Si heterojunctions exhibit good rectifying characteristics as traditional diodes.^{11,12} It is reported that they are sensitive to the light illumination and external magnetic field. Photovoltaic, photocurrent, and magnetoresistance effects have been observed in $\text{La}_{2/3}\text{Sr}_{1/3}\text{MnO}_{3-\delta}/\text{Si}$, $\text{La}_{0.6}\text{Ca}_{0.4}\text{MnO}_{3-\delta}/\text{Si}$, $\text{La}_{0.9}\text{Sr}_{0.1}\text{MnO}_3/\text{Si}$, $\text{La}_{0.67}(\text{Ca}_{0.75}\text{Ba}_{0.25})_{0.33}\text{MnO}_{3-\delta}/\text{Si}$.^{13–16} Theoretically, doping by tetravalent ions (such as Sn^{4+} , Ce^{4+} , Te^{4+} , and Zr^{4+}) result in n -type LaMnO_3 , and a few reports discuss their electron-type doping.^{17–19} However, it seems that

how to apply such n -type LaMnO_3 into device is a big challenge. To date, the relative reports are rather rare. Mitra *et al.* constructed a $p\text{-La}_{0.7}\text{Ca}_{0.3}\text{MnO}_3/i\text{-SrTiO}_3/n\text{-La}_{0.7}\text{Ce}_{0.3}\text{MnO}_3$ diode and observed asymmetric current-voltage characteristic.²⁰ Chou *et al.* observed the magnetoresistance in $\text{La}_{0.7}\text{Ce}_{0.3}\text{MnO}_3/\text{La}_{0.7}\text{Ca}_{0.3}\text{MnO}_3$ p - n junction.²¹

In the previous works of our group, it is found that Hf^{4+} -dopant can lead to reliable n -type LaMnO_3 .^{22,23} In this work, we fabricate heterojunctions of $n\text{-La}_{0.9}\text{Hf}_{0.1}\text{MnO}_3/p\text{-Si}$. In order to get high-quality epitaxial $\text{La}_{0.9}\text{Hf}_{0.1}\text{MnO}_3$ (LHMO) films, we prepared a 2-nm-thick SrTiO_3 (STO) buffer layer on the Si substrate. The junctions show good rectifying characteristic in a temperature range of 20 to 300 K. It is interesting that the reverse electrical transport is very sensitive to visible light illumination. The photo-induced effect exhibits strong dependence on the light intensity, bias voltage, and temperature.

The epitaxial LHMO films were grown on STO-buffered p -type Si (001) (ρ : $\sim 12 \Omega \text{ cm}$, size: $5 \times 5 \times 1 \text{ mm}^3$) substrates by pulse laser deposition technique. A pulsed laser beam (wavelength: 308 nm, repetition: 2 Hz, energy density: $\sim 1.5 \text{ J cm}^{-2}$) was focused on a sintered LHMO target. The distance of target-to-substrate was 50 mm. The temperature of the substrate was kept at 720°C and the oxygen pressure of the chamber was maintained at 2 Pa during the film growth. To enhance the crystalline quality, the samples were *in situ* annealed in 10^3 Pa high-purity oxygen for 1 h, and then cooled down to room temperature naturally. The preparation of STO layer on Si substrate had been described elsewhere.^{24–26} The thickness of LHMO film was about 150 nm measured by step profiler.

X-ray diffraction (XRD) with Cu $K\alpha$ radiation was used to determine the crystal structure of LHMO films. Keithley 2400 SourceMeter was employed to the electrical measurements. Ag electrodes with the area of 0.2 mm^2 were prepared by thermal evaporation. Temperature-dependent resistance

^{a)}Authors to whom correspondence should be addressed. Electronic addresses: hblu@iphy.ac.cn and jugao@hku.hk

of the LHMO film was measured by four-probe method. The current-voltage (I - V) characteristics of the LHMO/STO/Si heterojunctions were measured by traditional two-probe method at various temperatures. Semiconductor lasers with wavelengths of 630 and 532 nm with variable power density were employed to investigate the photo-induced effects.

XRD θ - 2θ scan profile of the LHMO film is shown in Figure 1. Only diffraction peaks from Si (001) and LHMO (001) planes are observed on the curve, meaning that the LHMO film grows along c -axis direction and is of single phase. The full width at half maximum of LHMO (002) peak is 0.35° , suggesting a good crystallinity. And the out-of-plane lattice parameter is reckoned to be $c = 3.908 \text{ \AA}$. The XRD signals of STO layer are submerged into the peaks of LHMO. In-plane resistance measurement of the LHMO film shows an ordering temperature around 250 K, as shown in the inset, where an iconic metal-insulator transition of manganite takes place. It also indicates the good crystallization.

I - V relationship of LHMO/STO/Si heterojunction was measured by tuning the applied voltage in a wide range. A schematic illustration of the sample is shown in the inset of Figure 2. The positive bias (forward bias) is defined as the current flows from Si to LHMO. Figure 2 plots the I - V curves measured at different temperature. Typically rectifying behaviors are observed in the LHMO/STO/Si heterojunction in the temperature range of 20–300 K in light of the severe asymmetry of the measured I - V curves, which is similar to the conventional p - n diodes.^{27,28} Leakage current occurring in the reverse bias region is very small and increases with the increasing temperature. It is only $110 \mu\text{A}$ at the bias of -10 V at 300 K. In contrast, with the increasing positive bias voltage, the currents begin to increase sharply at threshold voltages (or diffusion potential, V_D), herein, the values of V_D are about 0.6 V at each temperature. It seems that temperature has little impact on V_D . It should be noted that the diffusion potential is closed to the reported values of p -manganite/insulator/ n -Si junctions.^{11,29}

A fact should be noted, the electrical contact between Ag electrode and p -Si is not perfect Ohmic contact, the dashed line in Figure 2 presents the I - V curve of Ag/ p -Si/Ag (at 300 K) measured by two-probe method. However, we can see

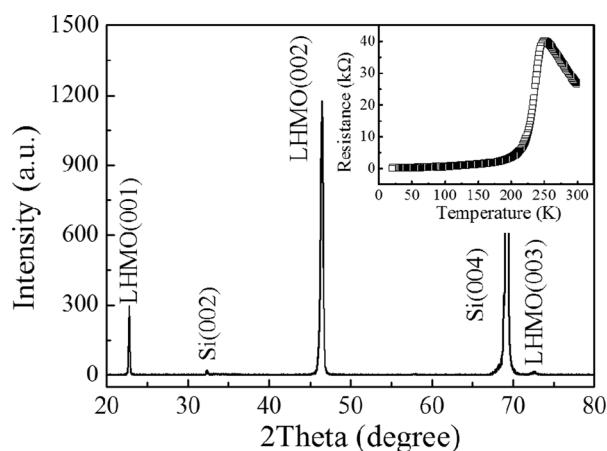


FIG. 1. XRD θ - 2θ profile of the LHMO film grown on Si (001) substrate with 2-nm-thick STO interlayer. The inset shows the temperature-dependent resistance of LHMO film.

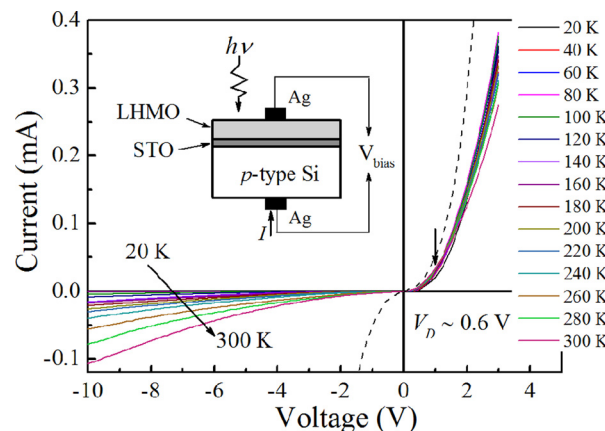


FIG. 2. The I - V curves of LHMO/STO/Si junction at different temperatures. The dash line shows I - V curve of Ag/ p -Si/Ag junction. The inset is a schematic illustration of the junction.

that contact potential of Ag/ p -Si provides negligible contribution to the rectifying behavior in Ag/LHMO/STO/Si/Ag structure. Therefore, the well rectifying property strongly suggests the formation of n - i - p junction in $\text{La}_{0.9}\text{Hf}_{0.1}\text{MnO}_3/\text{SrTiO}_3/\text{Si}$ system. For comparison, we also prepare a $\text{La}_{0.9}\text{Sr}_{0.1}\text{MnO}_3/\text{SrTiO}_3/\text{Si}$ sample under the same conditions, but poor rectifying characteristic is exhibited. Furthermore, it is insensitive to light illumination, which may be mainly from the contact potential between Ag electrode and Si substrate.

As well known, light illumination is an effective way to modulate the concentration of carriers in semiconductor materials and heterostructures. Photoinduced effects, such as photoconductivity and photovoltaic, are always the interesting topics in the research of manganites.^{9,30} We illuminate the surface of LHMO by 630 nm light (as shown in the inset of Figure 2) with different energy densities at room temperature, and the photo-effected I - V curves are displayed in Figure 3(a). It is obvious that the photoinduced effects on electrical transport are quite different under forward and reverse bias. The conductivity under forward bias is insensitive to the light, only finite changes in currents are detected. On the contrary, in the reverse bias region, the I - V responses show high sensitivity to the red light. Weak light of $P = 0.2 \text{ mW cm}^{-2}$ (P is power density) can enhance the leakage current (reverse current) observably. As the power density increases further, the reverse currents increase manifold. The reverse current increases over $700 \mu\text{A}$ under $P = 10 \text{ mW cm}^{-2}$ and $V_{\text{bias}} = -10 \text{ V}$. We also observed that the illumination of 532 nm light can lead to the same phenomenon. Sheng *et al.* observed similar phenomenon in $\text{Pr}_{0.7}\text{Ca}_{0.3}\text{MnO}_{3-\delta}/\text{SiO}_2/n$ -Si and $\text{La}_{0.67}\text{Sr}_{0.33}\text{MnO}_{3-\delta}/\text{SiO}_2/n$ -Si heterojunctions.³¹ Figure 3(b) shows the relationship between light power intensity and reverse current at certain voltages of 0 to -10 V . The solid lines are linear fitting results. The photocurrent increases linearly with the light power density. Meanwhile, the variation speed depends upon the sampling voltage strongly, as shown in the inset of Figure 3(b).

We use photosensitivity (I_S) to express the relative changes of the reverse currents, which is defined as $|I_{\text{Light}} - I_{\text{Dark}}|/|I_{\text{Dark}}| \times 100\%$, where I_{Light} and I_{Dark} are the photocurrent and dark current of the junction, respectively. Figure 3(c) displays I_S as a function of the reverse bias at certain light power densities, which shows I_S not only relates to the

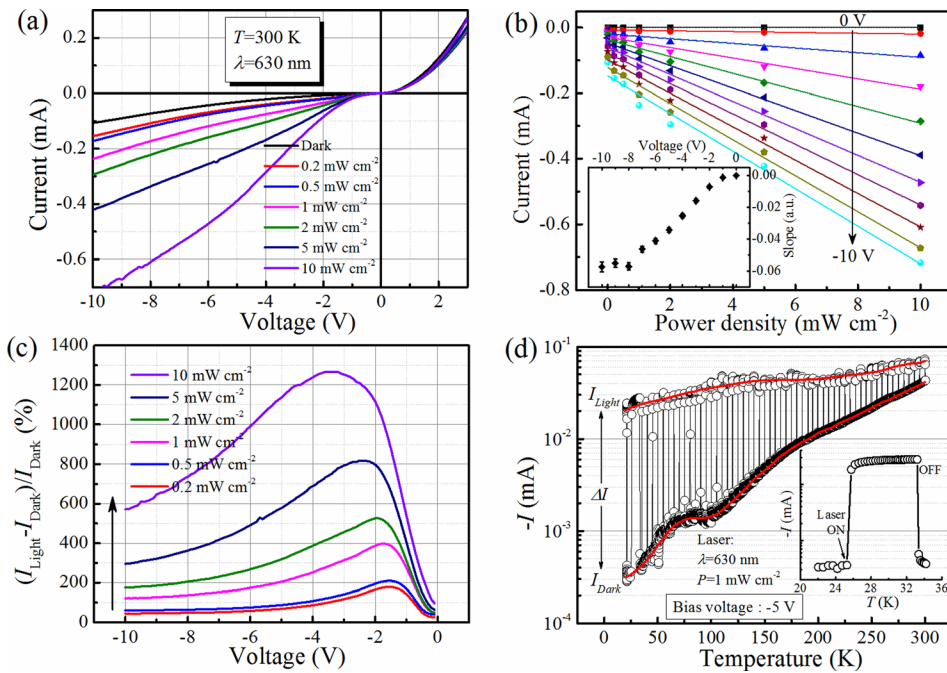


FIG. 3. (a) I - V responses of the LHMO/STO/Si junction under the illumination of 630 nm light with different energy densities at room temperature. (b) The relationship between light power intensity and reverse current at certain voltage of 0 to -10 V, the inset shows the slopes of the fitting lines. (c) The bias dependent photosensitivity (I_S) in the inverse bias region under the illumination of 630 nm laser with different energy densities. (d) Temperature-dependent currents under a sampling voltage of -5 V in the temperature range of 20–300 K, and 630 nm light with energy density of 1 mW cm^{-2} was illuminated on the LHMO for ~ 2 s for a temperature interval of 5 K, the lower circles are the currents in the dark, while the upper circles are the values under illumination. The solid lines are guides to eyes. The inset shows a complete circle composed of laser “ON” and “OFF.”

power density but also depends on bias voltage. It increases quickly as the reverse bias increased first, then begins to drop after increasing up to a maximum value. The maximum value shifts to the high bias voltage direction under the illumination of higher power density light. It is observed that 0.2 mW cm^{-2} red light almost triples the reverse current under -1.5 V bias, and I_S reaches over 1200% under -3 V bias when the power density is 10 mW cm^{-2} . It is conceivable, the magnitude of I_S at low temperature should be larger than those at high temperatures. As the temperature reduces to 200 K and 100 K, the maxima of I_S are 1800% and 13 000%, respectively. If cooling the sample to 20 K, I_S can reach as high as $10^7\%$, but we should note that the leakage currents are very close to zero at such low temperatures.

Figure 3(d) shows a dynamic current-temperature (I - T) relation of the junction under -5 V sampling voltage, and 1 mW cm^{-2} red light was illuminated on the sample at a temperature interval of 5 K in the heating process, the light duration was about 2 s. The lower and upper groups of circles are the currents recorded in the dark and under illumination, respectively. The inset of Figure 3(d) plots a complete circle composed of both laser “ON” and “OFF” actions, and its illumination time is about 120 s. We can clearly see the fast growth and decay processes of photoinduced current. There are two points should be noted in Figure 3(d). First, both I_{Dark} and I_{Light} increase with elevating temperature monotonously. Second, just as our expectation, the change of the currents (ΔI) increases when the temperature is decreased. At 300 K, the current only increases approximately two times; but at 20 K, the change of current has two orders of magnitude. The measurement in the same process with the illumination of 532 nm light shows similar result.

To understand the observed phenomenon, band model of heterojunction should be invoked. Figure 4(a) shows a schematic band diagram of the LHMO/STO/Si junction at equilibrium state. STO interlayer broadens the transition region. We suppose that most of the depletion region is

located at Si side.^{5,32} When a positive bias is applied on the junction, the current passing across the junction mainly comes from the diffusion of majority carriers (electrons in LHMO and holes in Si). At present, if red light illuminates on the surface of LHMO, a great part of the incident photons are absorbed by LHMO layer, electron-hole pairs form in LHMO since the photon energy is larger than the bandgaps of LHMO ($\sim 1.1 \text{ eV}$). Due to the action of external electric field, photogenerated holes are driven to the negative electrode on the surface of LHMO film and probably recombined

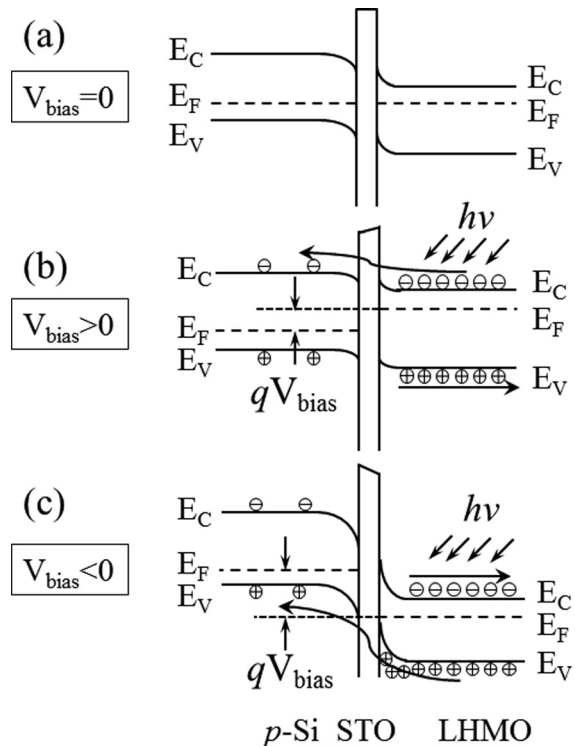


FIG. 4. Schematic energy band diagram for $\text{La}_{0.9}\text{Hf}_{0.1}\text{MnO}_3/\text{SrTiO}_3/\text{Si}$ p - i - n heterojunction with $V_{\text{bias}} = 0 \text{ V}$ and dark (a), $V_{\text{bias}} > 0 \text{ V}$ and illumination (b), and $V_{\text{bias}} < 0 \text{ V}$ and illumination (c).

with electrons in LHMO, meanwhile photogenerated electrons are driven across the junction into the Si, as the schematic diagram shown in Figure 4(b). The total junction current density includes three parts: $J = J_p(h) + J_n(e) + J_L(e)$, where $J_p(h)$ and $J_n(e)$ are current densities due to the diffusions of holes in Si and electrons in LHMO, $J_L(e)$ is the current density due to photogenerated electrons. But $J_L(e)$ is far less than $J_p(h)$ and $J_n(e)$ because the quantity of photogenerated electrons is too small in comparison with majority carriers in the sample. Therefore, $J_L(e)$ cannot increase J markedly. That is the reason why light illumination hardly influences the positive current.

But the situation is absolutely different when a reverse bias is applied on the junction. Without light illumination, the minority carriers (holes in LHMO and electrons in Si) drift across the junction to form the reverse current. Figure 4(c) shows the schematic energy band of the junction under reverse bias and light illumination. Photogenerated electrons are extracted out by the applied electric field. But photogenerated holes accumulate at the edge of space charge region on the LHMO side and drift across the junction. Then, the junction current density under light illumination can be written as $J = J_p(e) + J_n(h) + J_L(h)$, where $J_p(e)$ and $J_n(h)$ are current densities due to the drifts of electrons in p -Si and holes in n -LHMO, $J_L(h)$ is the current density from photogenerated holes. In fact, $J_p(e)$ and $J_n(h)$ are very small since the low concentration of minority carriers in semiconductor material. The quantity of photogenerated holes may be of the same order as that of minority carrier, even larger than minority carrier under bright enough light. In this case, slight change of $J_L(h)$ influences J considerably. In other words, light illumination can increase the reverse current signally.

Generally, $J_L(h)$ is in direct proportion to light intensity since higher light intensity produces more photogenerated holes, so J should increase with the increasing light intensity, meaning that larger photocurrent can be induced accordingly. Furthermore, the junction current density in the dark under reverse bias follows the relationship of $J \propto \exp(-I/k_0T)$. But the impact of temperature on $J_L(h)$ is small. Thus, the ratio of $J_L(h):(J_p(e) + J_n(h))$ should increase with decreasing temperature, indicating that the photosensitivity at low temperature is larger than that at high temperature. Here, we just make a possible qualitative explanation to the photocurrent, and more accurate interpretation relies on further studies.

The observed photocurrent makes the LHMO/STO/Si heterojunctions to be good photo detector. At first, we explore the temporal recovery of conductivity at room temperature. Figure 5(a) plots the photocurrents as a function of time while the lasers are switched on and off. The currents abruptly hop to a high level as soon as the lights illuminate on the junction and keep at least 1800 s. The currents almost recover to the initial stage immediately once switching off the lasers. Good repeatability is an important standard for a device. Figure 5(b) shows the photocurrent responses for ten cycles. It shows quick switch between small and large currents corresponding to “light ON” and “light OFF” states, respectively, indicating reliable photo detection behavior. According to the mechanism of photocurrent in the LHMO/STO/Si structure, this detector can response for the lights

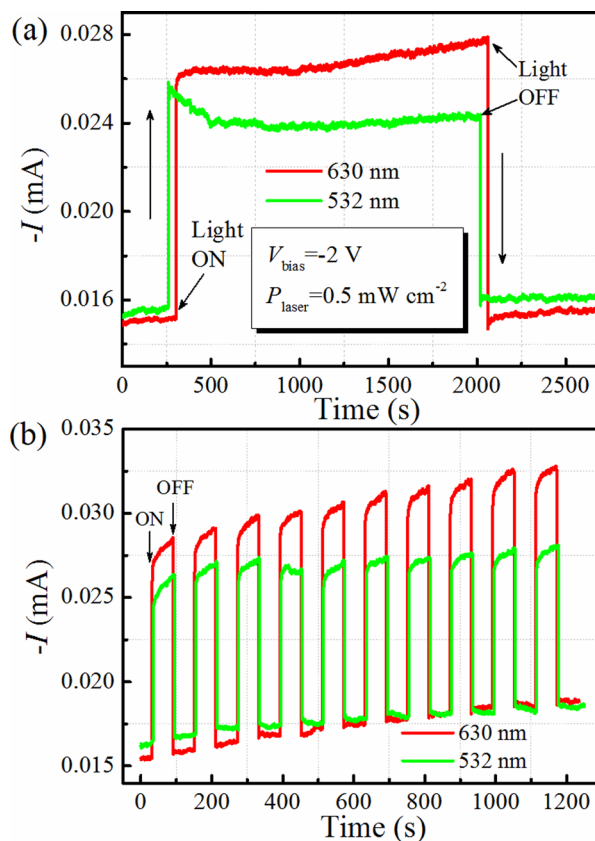


FIG. 5. (a) Current versus illumination time for the LHMO/STO/Si heterojunction, showing persistent photocurrent. (b) Responses of photocurrent to the intermittent light illumination (wavelength: 630 nm and 532 nm, power density: 0.5 mW cm^{-2} , sampling voltage: -2 V , temperature: 300 K).

whose energy is larger than the bandgap of LHMO, so it is foreseeable that it must be a good detector for visible and ultraviolet lights.

In conclusion, LHMO/STO/Si heterojunctions were fabricated by PLD method. The junctions exhibited an excellent rectifying characteristic in a wide temperature range. Most interestingly, the electrical transport under reverse bias was sensitive to visible light. Large photocurrent was observed when monochromatic light illuminated on the LHMO surface. The photocurrent was influenced by light intensity, bias voltage, and temperature. The different effect of positive and reverse bias on the photogenerated carriers was the possible reason to the observed phenomenon. The results reveal the feasible manipulation to electrical transport of manganite/insulator/Si heterojunction by light illumination and bias voltage, and suggest that LHMO/STO/Si can be good electronic and optoelectronic devices.

This work has been supported by the National Key Project for Basic Research of China (No. 2014CB921002), the National Natural Science Foundation of China (Grant No. 11374225), and the Research Grant Council of Hong Kong (Project Code No. 702112).

¹M. B. Salamon and M. Jaime, *Rev. Mod. Phys.* **73**(3), 583 (2001).

²J. H. Song, T. Susaki, and H. Y. Hwang, *Adv. Mater.* **20**(13), 2528–2532 (2008).

³V. Kiryukhin, D. Casa, J. Hill, B. Keimer, A. Vigliante, Y. Tomioka, and Y. Tokura, *Nature* **386**, 813–815 (1997).

- ⁴H. Lu, C. Zhang, H. Guo, H. Gao, M. Liu, J. Liu, G. Collins, and C. Chen, *ACS Appl. Mater. Interfaces* **2**(9), 2496–2499 (2010).
- ⁵J. Du, H. Ni, K. Zhao, Y.-C. Kong, H. Wong, S. Zhao, and S. Chen, *Opt. Express* **19**(18), 17260–17266 (2011).
- ⁶H. Lu, S. Dai, Z. Chen, Y. Zhou, B. Cheng, K. Jin, L. Liu, G. Yang, and X. Ma, *Appl. Phys. Lett.* **86**(3), 32502 (2005).
- ⁷J. Qiu, H.-B. Lu, K.-J. Jin, M. He, and J. Xing, *Physica B* **400**(1), 66–69 (2007).
- ⁸A. Congeduti, P. Postorino, E. Caramagno, M. Nardone, A. Kumar, and D. Sarma, *Phys. Rev. Lett.* **86**(7), 1251–1254 (2001).
- ⁹J. Dai, W. Song, S. Wang, S. Ye, K. Wang, J. Du, and Y. Sun, *J. Appl. Phys.* **90**(6), 3118–3120 (2001).
- ¹⁰X. Zhou, J. Xue, D. Zhou, Z. Wang, Y. Bai, X. Wu, X. Liu, and J. Meng, *ACS Appl. Mater. Interfaces* **2**(10), 2689–2693 (2010).
- ¹¹P. Lang, Y. Zhao, B. Yang, X. Zhang, J. Li, P. Wang, and D. N. Zheng, *Appl. Phys. Lett.* **87**(5), 053502 (2005).
- ¹²J. Gao and F. Hu, *Mat. Sci. Eng. B* **144**(1), 100–103 (2007).
- ¹³Z. Sheng, Y. Sun, J. Dai, X. Zhu, and W. Song, *Appl. Phys. Lett.* **89**(8), 082503 (2006).
- ¹⁴Z. Yan, X. Yuan, Y. Xu, G. Gao, K. Jin, and C. Chen, *J. Phys. D: Appl. Phys.* **40**(9), 2797 (2007).
- ¹⁵J. Xing, K. Zhao, G. Z. Liu, M. He, K. J. Jin, and H. B. Lu, *J. Phys. D: Appl. Phys.* **40**(19), 5892 (2007).
- ¹⁶Z. Yan, X. Yuan, X. Zhang, Y. Xu, and F. Wang, *J. Phys. D: Appl. Phys.* **41**(13), 135302 (2008).
- ¹⁷T. Cheng, C. Lin, L. Chang, C. Hsu, J. Lee, J. Chen, J.-Y. Lin, K. Wu, T. Uen, and Y. Gou, *Phys. Rev. B* **74**(13), 134428 (2006).
- ¹⁸H. Chou, C. Wu, S. Hsu, and C. Wu, *Phys. Rev. B* **74**(17), 174405 (2006).
- ¹⁹J. Gao, S. Dai, and T. Li, *Phys. Rev. B* **67**(15), 153403 (2003).
- ²⁰C. Mitra, P. Raychaudhuri, G. Kobernik, K. Dorr, R. Pinto, K. Muller, and L. Schultz, *Appl. Phys. Lett.* **79**, 2408 (2001).
- ²¹H. Chou, Z. Hong, S. Sun, J. Juang, and W. Chang, *J. Appl. Phys.* **97**(10), 10A308 (2005).
- ²²L. Wang and J. Gao, *J. Appl. Phys.* **105**, 07E514 (2009).
- ²³L. Wang and J. Gao, *J. Appl. Phys.* **105**, 07C904 (2009).
- ²⁴K. Zhao, Y. Huang, Q. Zhou, K.-J. Jin, H. Lu, M. He, B. Cheng, Y. Zhou, Z. Chen, and G. Yang, *Appl. Phys. Lett.* **86**(22), 221917 (2005).
- ²⁵H. Tian, H. Yang, H. Zhang, Y. Li, H. Lu, and J. Li, *Phys. Rev. B* **73**(7), 075325 (2006).
- ²⁶X. Zhou, J. Miao, J. Dai, H. L. Chan, C. Choy, Y. Wang, and Q. Li, *Appl. Phys. Lett.* **90**(1), 012902 (2007).
- ²⁷K. W. Böer, *Survey of Semiconductor Physics: Volume II Barriers, Junctions, Surfaces, and Devices* (Springer Science & Business Media, 2012).
- ²⁸S. M. Sze, *Semiconductor Devices: Physics and Technology* (John Wiley & Sons, 2008).
- ²⁹P. Lang, Y. Zhao, C. Xiong, P. Wang, J. Li, and D. Zheng, *J. Appl. Phys.* **100**(5), 053909 (2006).
- ³⁰Z. Luo and J. Gao, *J. Appl. Phys.* **100**(5), 056104 (2006).
- ³¹Z. Sheng, Y. Sun, J. Dai, X. Zhu, W. Song, and Z. Yang, *J. Phys. D: Appl. Phys.* **42**(8), 085002 (2009).
- ³²H. B. Lu, K. J. Jin, Y. H. Huang, M. He, K. Zhao, B. L. Cheng, Z. H. Chen, Y. L. Zhou, S. Y. Dai, and G. Z. Yang, *Appl. Phys. Lett.* **86**(24), 241915 (2005).